

# Spectroscopic Evidence for Argentophilicity in Structurally Characterized Luminescent Binuclear Silver(I) Complexes

Chi-Ming Che,\* Man-Chung Tse, Michael C. W. Chan, Kung-Kai Cheung, David Lee Phillips,\* and King-Hung Leung

Contribution from the Department of Chemistry, The University of Hong Kong, Pokfulam Road, Hong Kong SAR, China

Received February 16, 1999. Revised Manuscript Received November 22, 1999

**Abstract:** A spectroscopic and structural investigation of binuclear silver(I) complexes supported by aliphatic phosphine ligands, namely  $[\text{Ag}(\text{PCy}_3)(\text{O}_2\text{CCF}_3)]_2$  (**1**),  $[\text{Ag}_2(\mu\text{-dcpm})_2]\text{X}_2$  ( $\text{X} = \text{CF}_3\text{SO}_3$ , **2**;  $\text{PF}_6$ , **3**; dcpm = bis(dicyclohexylphosphino)methane), and  $[\text{Ag}_2(\mu\text{-dcpm})(\mu\text{-O}_2\text{CCF}_3)_2]$  (**4**), is described. X-ray structural analyses of **1–4** reveal Ag–Ag separations of 3.095(1), 2.948 (av), 2.923 (av), and 2.8892(9) Å, respectively. Due to the optical transparency of the phosphine ligands, the UV–vis absorption band at 261 nm in  $\text{CH}_3\text{CN}$  for **2** and **3** is assigned to a  $4d\sigma^* \rightarrow 5p\sigma$  transition originating from Ag(I)–Ag(I) interactions. The argentophilic nature of this band is verified by the resonance Raman spectrum of **2** with 273.9 nm excitation, where virtually all of the Raman intensity appears in the Ag–Ag stretch fundamental ( $80 \text{ cm}^{-1}$ ) and overtone bands. Complexes **2** and **3** exhibit photoluminescence in the solid state at room temperature.

## Introduction

The propensity for aggregation of formally closed-shell  $d^{10}$  metal ions in polynuclear coordination compounds and solid-state lattices has long been recognized and exploited in, inter alia, supramolecular assembly and the design of molecules with rich photophysical properties.<sup>1</sup> Model spectroscopic studies of  $d^{10}\text{–}d^{10}$  interactions in binuclear species, such as  $[\text{Au}_2(\text{dppm})_2]^{2+}$  (dppm = bis(diphenylphosphino)methane),<sup>2</sup> have established the occurrence of a low-energy  $nd\sigma^* \rightarrow (n+1)p\sigma$  transition that is absent in the mononuclear two-coordinate counterparts.<sup>3</sup> This type of transition was originally observed in the related  $d^8\text{–}d^8$  systems for Rh(I) and Pt(II) species by Gray and co-workers,<sup>4</sup> and is considered to be reliable evidence of weak metal–metal interaction in the ground state (and strong interaction in the excited state). While aurophilic attraction between gold(I) ions is widely acknowledged,<sup>5</sup> the development of silver–silver bonding interactions, or argentophilicity, remains in its infancy. Reports by Jansen of extended silver(I) aggregates in the ionic lattices of ternary silver(I) oxides and halides appeared over 10 years ago.<sup>1a</sup> More recently, silver nanoparticles with unique optical and electronic properties have been investigated in the emerging field of nanoscale materials.<sup>6</sup>

\* Corresponding authors. Fax: +852 2857 1586. E-mail: cmche@hku.hk or phillips@hku.hk.

(1) (a) Jansen, M. *Angew. Chem., Int. Ed. Engl.* **1987**, *26*, 1098–1110. (b) Pyykkö, P. *Chem. Rev.* **1997**, *97*, 597–636. (c) Schmidbaur, H. *Chem. Soc. Rev.* **1995**, *24*, 391–400. (d) Puddephatt, R. J. *Chem. Commun.* **1998**, 1055–1062.

(2) (a) Che, C. M.; Kwong, H. L.; Yam, V. W. W.; Cho, K. C. *J. Chem. Soc., Chem. Commun.* **1989**, 885–886. (b) King, C.; Wang, J. C.; Khan, Md. N. I.; Fackler, J. P., Jr. *Inorg. Chem.* **1989**, *28*, 2145–2149.

(3) (a) Caspar, J. V. *J. Am. Chem. Soc.* **1985**, *107*, 6718–6719. (b) Harvey, P. D.; Gray, H. B. *J. Am. Chem. Soc.* **1988**, *110*, 2145–2147.

(4) (a) Mann, K. R.; Gordon, J. G., II; Gray, H. B. *J. Am. Chem. Soc.* **1975**, *97*, 3553–3555. (b) Rice, S. F.; Gray, H. B. *J. Am. Chem. Soc.* **1983**, *105*, 4571–4575.

(5) Schmidbaur, H. *Gold Bull.* **1990**, *23*, 11–21.

(6) For recent examples, see: (a) Quaroni, L.; Chumanov, G. *J. Am. Chem. Soc.* **1999**, *121*, 10642–10643. (b) Markovich, G.; Collier, C. P.; Henrichs, S. E.; Remacle, F.; Levine, R. D.; Heath, J. R. *Acc. Chem. Res.* **1999**, *32*, 415–423.

For coordination compounds, accounts of ligand-unsupported Ag–Ag contacts based on structural determinations are scarce.<sup>7,8</sup> Short Ag(I)–Ag(I) separations ( $<3.4 \text{ Å}$ , sum of van der Waals radii<sup>9</sup>) in bi- and polynuclear complexes are typically maintained by bridging ligands, but whether this constitutes the existence of  $d^{10}\text{–}d^{10}$  interactions is yet to be resolved.<sup>10,11</sup> We now present the first unequivocal spectroscopic evidence for argentophilicity in binuclear silver(I) complexes bearing aliphatic phosphine ligands.

## Experimental Section

**General Procedures.** All reagents were obtained from commercial sources and all solvents used for reactions were of analytical grade and purified according to conventional methods. Details of solvent treatment for photophysical studies, instrumentation, and emission measurements have been provided earlier<sup>12</sup> and are given in the Supporting Information.  $[\text{Ag}_2(\mu\text{-dmpm})_2](\text{PF}_6)_2$  (dmpm = bis(dimethylphosphino)methane) was prepared by the literature method.<sup>13</sup>  $[\text{Ag}(\text{PR}_3)_2]\text{ClO}_4$  ( $\text{R} = \text{Me}, \text{Cy}$ ) was synthesized by interaction of the phosphine with  $\text{AgClO}_4$  and characterized by elemental analyses, <sup>31</sup>P NMR, and FAB mass spectroscopy. The resonance Raman apparatus and methods have previously been described in detail,<sup>14</sup> and a summary is given here. The second anti-stokes Raman shifted line of the third

(7) (a) Kim, Y.; Seff, K. *J. Am. Chem. Soc.* **1978**, *100*, 175–180. (b) Eastland, G. W.; Mazid, M. A.; Russell, D. R.; Symons, M. C. R. *J. Chem. Soc., Dalton Trans.* **1980**, 1682–1687. (c) Kappenstein, C.; Ouali, A.; Guerin, M.; Cernák, J.; Chomic, J. *Inorg. Chim. Acta* **1988**, *147*, 189–197. (d) Quirós, M. *Acta Crystallogr.* **1994**, *C50*, 1236–1239.

(8) (a) Singh, K.; Long, J. R.; Stavropoulos, P. *J. Am. Chem. Soc.* **1997**, *119*, 2942–2943. (b) Omary, M. A.; Webb, T. R.; Assefa, Z.; Shankle, G. E.; Patterson, H. H. *Inorg. Chem.* **1998**, *37*, 1380–1386.

(9) Bondi, A. J. *Phys. Chem.* **1964**, *68*, 441–451.

(10) Cotton, F. A.; Feng, X.; Matusz, M.; Poli, R. *J. Am. Chem. Soc.* **1988**, *110*, 7077–7083.

(11) (a) El-Bahraoui, J.; Molina, J.; Portal, D. *J. Phys. Chem. A* **1998**, *102*, 2443–2448. (b) Fernández, E. J.; López-de-Luzuriaga, J. M.; Monge, M.; Rodríguez, M. A.; Crespo, O.; Gimeno, M. C.; Laguna, A.; Jones, P. G. *Inorg. Chem.* **1998**, *37*, 6002–6006.

(12) Lai, S. W.; Chan, M. C. W.; Cheung, T. C.; Peng, S. M.; Che, C. M. *Inorg. Chem.* **1999**, *38*, 4046–4055.

(13) Karsch, H. H.; Schubert, U. Z. *Naturforsch.* **1982**, *37B*, 186–189.

(14) Zheng, X.; Phillips, D. L. *J. Chem. Phys.* **1998**, *108*, 5772–5783.

Table 1. Crystal Data

	1	2	3	4
formula	C <sub>40</sub> H <sub>66</sub> O <sub>4</sub> Ag <sub>2</sub> F <sub>6</sub> P <sub>2</sub>	C <sub>52</sub> H <sub>92</sub> O <sub>6</sub> Ag <sub>2</sub> F <sub>6</sub> P <sub>4</sub> S <sub>2</sub>	C <sub>50</sub> H <sub>92</sub> Ag <sub>2</sub> F <sub>12</sub> P <sub>6</sub>	C <sub>29</sub> H <sub>46</sub> O <sub>4</sub> Ag <sub>2</sub> F <sub>6</sub> P <sub>2</sub>
fw	1002.63	1331.04	1322.84	850.35
crystal system	monoclinic	monoclinic	monoclinic	monoclinic
space group	C2/c (No. 15)	P2 <sub>1</sub> /c	P2 <sub>1</sub> /a (No. 14)	P2 <sub>1</sub> /n (No. 13)
color	colorless	colorless	colorless	colorless
crystal size, mm	0.40 × 0.20 × 0.10	0.35 × 0.25 × 0.15	0.25 × 0.20 × 0.08	0.30 × 0.25 × 0.15
a, Å	27.074(3)	22.873(3)	18.572(4)	13.205(3)
b, Å	9.649(2)	16.540(3)	14.758(3)	9.109(3)
c, Å	18.948(3)	17.502(4)	22.858(4)	14.327(3)
β, deg	119.34(2)	110.05(2)	108.14(2)	92.76(2)
V, Å <sup>3</sup>	4314(1)	6220(2)	5953(1)	1721.4(6)
T, K	301	298	301	301
Z	4	4	4	2
D <sub>c</sub> (g cm <sup>-3</sup> )	1.543	1.421	1.476	1.640
μ, cm <sup>-1</sup>	10.43	8.59	8.87	12.91
F(000)	2064	2768	2736	860
2θ <sub>max</sub> , deg	52	44	51	50
R, <sup>a</sup> R <sub>w</sub> <sup>b</sup>	0.067, 0.091	0.055, 0.084	0.066, 0.108	0.033, 0.042
residual ρ, e Å <sup>-3</sup>	+1.05, -0.85	+1.38, -1.54	+1.07, -1.04	+0.76, -0.41

$${}^a R = \sum ||F_o| - |F_c|| / \sum |F_o|. \quad {}^b R_w = [\sum w(|F_o| - |F_c|)^2 / \sum w|F_o|^2]^{1/2}.$$

harmonic of a Nd:YAG laser provided the excitation frequency for the resonance Raman experiment. The laser beam was loosely focused onto the sample using ~130° backscattering geometry and reflective optics were used to collect the Raman scattered light and image it through a depolarizer and entrance slit of a 0.5 m spectrometer. The grating of the spectrometer dispersed the Raman light onto a liquid nitrogen cooled CCD detector. Accumulations of about 1 min were acquired from the CCD and about 30 of these scans were added up to find the resonance Raman spectrum. Known acetonitrile solvent bands and Hg lamp emission lines were used to calibrate the Raman shifts of the resonance Raman spectrum. Appropriately scaled solvent and quartz cell background spectra (accumulated simultaneously with the sample spectra on a different part of the CCD) were subtracted to remove the solvent bands, the Rayleigh line, and the quartz cell background signal from the resonance Raman spectrum.

**Syntheses. (a) [Ag(PCy<sub>3</sub>)(O<sub>2</sub>CCF<sub>3</sub>)<sub>2</sub>] (1).** A CH<sub>2</sub>Cl<sub>2</sub> solution (30 mL) of Ag(O<sub>2</sub>CCF<sub>3</sub>) (0.10 g, 0.45 mmol) and tricyclohexylphosphine (0.13 g, 0.45 mmol) was stirred at room temperature for 6 h. A white solid was afforded upon precipitation by *n*-hexane. Recrystallization from a mixture of CH<sub>2</sub>Cl<sub>2</sub>/*n*-hexane yielded colorless rods. Yield: 0.19 g, 85%. Mp 177–178 °C. MS-FAB (+ve, *m/z*): 1003 (M<sup>+</sup>), 501 (M<sup>+</sup>/2). <sup>31</sup>P{<sup>1</sup>H} NMR (202 MHz, CDCl<sub>3</sub>): δ 30.4 (dm, *J* = 580 Hz). FT-IR (KBr, cm<sup>-1</sup>): 2988s, 1712s, 1450m, 1418m, 1021s, 950m, 761m, 691s, 600m, 555s. Anal. Calcd for C<sub>40</sub>H<sub>66</sub>O<sub>4</sub>Ag<sub>2</sub>F<sub>6</sub>P<sub>2</sub>: C, 47.92; H, 6.63. Found: C, 47.85; H, 6.54.

**(b) [Ag<sub>2</sub>(μ-dcpm)<sub>2</sub>](CF<sub>3</sub>SO<sub>3</sub>)<sub>2</sub> (2).** Bis(dicyclohexylphosphino)methane (0.16 g, 0.40 mmol) and a suspension of Ag(CF<sub>3</sub>SO<sub>3</sub>) (0.10 g, 0.39 mmol) in dichloromethane (30 mL) was stirred for 6 h. A white solid was afforded upon precipitation by diethyl ether. Recrystallization by diffusion of diethyl ether into an acetonitrile solution gave colorless crystals. Yield: 0.23 g, 90%. Mp 210–212 °C. MS-FAB (+ve, *m/z*): 1033 (M<sup>+</sup>). <sup>31</sup>P{<sup>1</sup>H} NMR (202 MHz, CDCl<sub>3</sub>): δ 33.9 (dm, *J* = 660 Hz). FT-IR (KBr, cm<sup>-1</sup>): 2989s, 1480m, 1423m, 1008s, 948s, 725m, 633m, 501s. Anal. Calcd for C<sub>52</sub>H<sub>92</sub>O<sub>6</sub>Ag<sub>2</sub>F<sub>6</sub>P<sub>4</sub>S<sub>2</sub>: C, 46.92; H, 6.97. Found: C, 46.98; H, 6.89.

**(c) [Ag<sub>2</sub>(μ-dcpm)<sub>2</sub>](PF<sub>6</sub>)<sub>2</sub> (3).** A suspension of AgPF<sub>6</sub> (0.10 g, 0.40 mmol) in dichloromethane (40 mL) and bis(dicyclohexylphosphino)methane (0.16 g, 0.40 mmol) was stirred at 40 °C for 5 h. Upon concentration and addition of diethyl ether, a white crystalline solid was obtained. Recrystallization by diffusion of diethyl ether into a dichloromethane solution afforded colorless crystals. Yield: 0.24 g, 92%. Mp 236–237 °C. MS-FAB (+ve, *m/z*): 1033 (M<sup>+</sup>). <sup>31</sup>P{<sup>1</sup>H} NMR (202 MHz, CDCl<sub>3</sub>): δ 36.3 (dm, *J* = 690 Hz). FT-IR (KBr, cm<sup>-1</sup>): 3001s, 1475m, 1401m, 1004vs, 977s, 745m, 622m. Anal. Calcd for C<sub>50</sub>H<sub>92</sub>Ag<sub>2</sub>F<sub>12</sub>P<sub>6</sub>: C, 45.40; H, 7.01. Found: C, 45.56; H, 6.95.

**(d) [Ag<sub>2</sub>(μ-dcpm)(μ-O<sub>2</sub>CCF<sub>3</sub>)<sub>2</sub>] (4).** A suspension of Ag(O<sub>2</sub>CCF<sub>3</sub>) (0.15 g, 0.68 mmol) and bis(dicyclohexylphosphino)methane (0.14 g, 0.34 mmol) in dichloromethane was stirred for 5 h. Removal of volatile

components yielded a white crystalline solid. The crude product was recrystallized by vapor diffusion of diethyl ether into a dichloromethane solution to afford colorless crystals. Yield: 0.21 g, 73%. Mp 222–223 °C. MS-FAB (+ve, *m/z*): 850 (M<sup>+</sup>). <sup>31</sup>P{<sup>1</sup>H} NMR (202 MHz, CDCl<sub>3</sub>): δ 35.0 (dm, *J* = 660 Hz). FT-IR (KBr, cm<sup>-1</sup>): 2990s, 1701s, 1469m, 1420m, 1010s, 930s, 752m, 603m, 543s. Anal. Calcd for C<sub>29</sub>H<sub>46</sub>O<sub>4</sub>Ag<sub>2</sub>F<sub>6</sub>P<sub>2</sub>: C, 40.96; H, 5.45. Found: C, 40.79; H, 5.59.

**X-ray Crystallography.** Crystal data and details of collection and refinement are summarized in Table 1. For 1/3 respectively, a total of 4085/10929 unique reflections were collected on a MAR diffractometer with a 300 nm image plate detector [ $\lambda$ (Mo K $\alpha$ ) = 0.71073 Å]. The structures were solved by direct methods (SIR92<sup>15</sup>), expanded using Fourier techniques, and refined by full-matrix least squares using the TeXsan<sup>16</sup> software package for 3012/6074 reflections with *I* > 3σ(*I*) and 244/599 parameters. For 2/4 respectively, a total of 8069/3248 unique reflections were collected on a Nonius CAD4/Rigaku AFC7R diffractometer [ $\lambda$ (Mo K $\alpha$ ) = 0.71073 Å, ω – 2θ scans]. The structures were solved by Patterson<sup>17</sup>/direct<sup>15</sup> methods, expanded using Fourier techniques, and refined by full-matrix least squares using the TeXsan<sup>16</sup> software package for 5838/2267 absorption-corrected (transmission 0.91–1.00/0.85–1.00) reflections with *I* > 3σ(*I*) and 649/195 parameters.

## Results and Discussion

**Synthesis and Structural Characterization.** Reaction of stoichiometric amounts of Ag(O<sub>2</sub>CCF<sub>3</sub>) with tricyclohexylphosphine (PCy<sub>3</sub>) in CH<sub>2</sub>Cl<sub>2</sub> afforded colorless crystals of [Ag(PCy<sub>3</sub>)(O<sub>2</sub>CCF<sub>3</sub>)<sub>2</sub>] (1, 85%) upon recrystallization from CH<sub>2</sub>Cl<sub>2</sub>/*n*-hexane. Similarly, treatment of AgX (X = O<sub>3</sub>SCF<sub>3</sub> and PF<sub>6</sub>) with bis(dicyclohexylphosphino)methane (dcpm) in CH<sub>2</sub>Cl<sub>2</sub> gave [Ag<sub>2</sub>(μ-dcpm)<sub>2</sub>]X<sub>2</sub> as colorless solids [X = CF<sub>3</sub>SO<sub>3</sub> (2, 90%), PF<sub>6</sub> (3, 87%)] which can be recrystallized from CH<sub>3</sub>CN/Et<sub>2</sub>O for 2 and CH<sub>2</sub>Cl<sub>2</sub>/Et<sub>2</sub>O for 3, respectively. The bis(trifluoroacetate) species [Ag<sub>2</sub>(μ-dcpm)(μ-O<sub>2</sub>CCF<sub>3</sub>)<sub>2</sub>] (4, 73%) was formed by interaction of 2 molar equiv of Ag(O<sub>2</sub>CCF<sub>3</sub>) with dcpm. All four complexes displayed distinctive doublets of multiplets in their <sup>31</sup>P{<sup>1</sup>H} NMR spectra at δ 30–36 in CDCl<sub>3</sub>.

(15) SIR92: Altomare, A.; Cascarano, M.; Giacovazzo, C.; Guagliardi, A.; Burla, M. C.; Polidori, G.; Camalli, M. *J. Appl. Crystallogr.* **1994**, *27*, 435.

(16) TeXsan: *Crystal Structure Analysis Package*; Molecular Structure Corporation: The Woodlands, TX, 1985 and 1992.

(17) PATTY: Beurskens, P. T.; Admiraal, G.; Beurskens, G.; Bosman, W. P.; Garcia-Granda, S.; Gould, R. O.; Smits, J. M. M.; Smykalla, C. The DIRDIF program system, Technical Report of the Crystallography Laboratory, University of Nijmegen, The Netherlands, 1992.

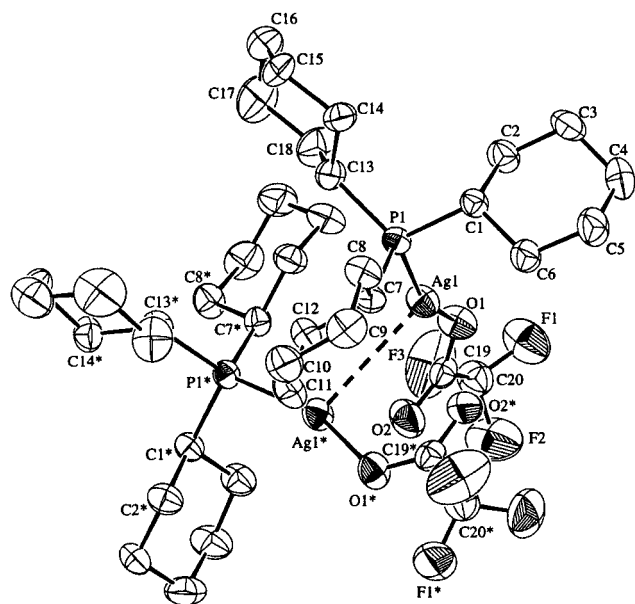


**Figure 1.** Perspective view of  $[\text{Ag}(\text{PCy}_3)(\text{O}_2\text{CCF}_3)]_2$ , **1** (40% thermal ellipsoids). Selected bond distances (Å) and angles (deg):  $\text{Ag}(1)-\text{Ag}(1^*)$  3.095(1),  $\text{Ag}(1)-\text{O}(1)$  2.173(5),  $\text{Ag}(1)-\text{O}(2^*)$  2.509(6),  $\text{Ag}(1)-\text{P}(1)$  2.377(2),  $\text{O}(1)-\text{C}(19)$  1.202(9);  $\text{Ag}(1^*)-\text{Ag}(1)-\text{O}(1)$  85.4(1),  $\text{Ag}(1^*)-\text{Ag}(1)-\text{P}(1)$  110.57(5),  $\text{P}(1)-\text{Ag}(1)-\text{O}(1)$  160.7(2),  $\text{Ag}(1)-\text{O}(1)-\text{C}(19)$  123.7(5).

Compounds **1–4** have been characterized by X-ray crystallography. Complex **1** crystallizes in a dimeric form, with two  $[(\text{Cy}_3\text{P})\text{Ag}(\text{O}_2\text{CCF}_3)]$  units ( $\text{P}-\text{Ag}-\text{O} = 160.7(2)^\circ$ ) held together by an  $\text{Ag}-\text{Ag}$  contact of 3.095(1) Å (Figure 1). The  $\text{PCy}_3$  and trifluoroacetate ligands are in a syn configuration, with  $\text{Ag}-\text{O}(\text{acetate})$  distances of 2.173(5) and 2.509(6) Å. The crystal structure of the phosphine-bridged derivative  $[\text{Ag}_2(\mu\text{-dcpm})(\mu\text{-O}_2\text{CCF}_3)_2]$  (**4**, Figure 3) also reveals short and long  $\text{Ag}-\text{O}(\text{acetate})$  separations (2.191(3) and 2.446(4) Å respectively), plus a silver-silver distance of 2.8892(9) Å.

The molecular structures of **2** and **3** (Figure 2) contain  $\text{Ag}_2\text{P}_4\text{C}_2$  cores that adopt chair conformations. The silver-silver separations of 2.936(1) and 2.960(1) Å in **2** and 2.907(1) and 2.938(1) Å in **3**, plus those in **1** and **4**, are typical for polynuclear  $\text{Ag}(\text{I})$  derivatives with proposed  $d^{10}-d^{10}$  interactions.<sup>7,8,18</sup> A slightly longer  $\text{Ag}-\text{Ag}$  distance of 3.041(2) Å was reported for the analogous complex  $[\text{Ag}_2(\mu\text{-dmpm})_2](\text{PF}_6)_2$ .<sup>13</sup> Close cation-anion contacts are evident in the crystal lattices of **2** (e.g.  $\text{Ag}(1)\cdots\text{O}(3)$  2.692(7) Å) and **3** (e.g.  $\text{Ag}(1)\cdots\text{F}(2')$  2.64(5) Å), but intriguingly, such interactions are not apparent in the X-ray structure<sup>19</sup> of the gold(I) congener  $[\text{Au}_2(\mu\text{-dcpm})_2](\text{ClO}_4)_2$  (closest  $\text{Au}\cdots\text{OClO}_3$  3.36(2) Å).

**Spectroscopic Characterization.** Previous assignments of the metal-centered  $4d\sigma^* \rightarrow 5p\sigma$  transition in polynuclear silver(I) compounds with bridging arylphosphine ligands are problematic because the intraligand transitions of free arylphosphines

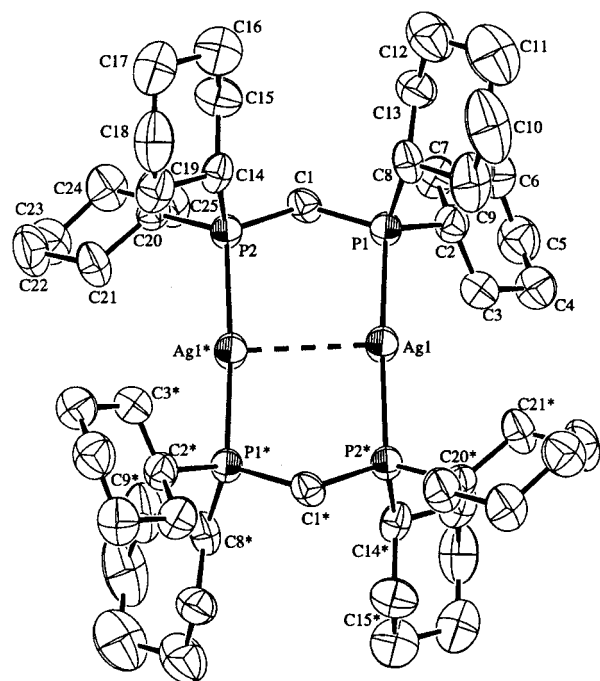


**Figure 2.** Perspective view of cation **1** in  $[\text{Ag}_2(\mu\text{-dcpm})_2](\text{PF}_6)_2$ , **3** (40% thermal ellipsoids). Selected bond distances (Å) and angles (deg):  $\text{Ag}(1)-\text{Ag}(1^*)$  2.938(1),  $\text{Ag}(1)-\text{P}(1)$  2.405(2),  $\text{Ag}(1)-\text{P}(2^*)$  2.405(2);  $\text{Ag}(1^*)-\text{Ag}(1)-\text{P}(1)$  92.89(5),  $\text{Ag}(1^*)-\text{Ag}(1)-\text{P}(2^*)$  90.69(5),  $\text{P}(1)-\text{Ag}(1)-\text{P}(2^*)$  172.37(8),  $\text{Ag}(1)-\text{P}(1)-\text{C}(1)$  111.9(2),  $\text{P}(1)-\text{C}(1)-\text{P}(2)$  114.5(4).

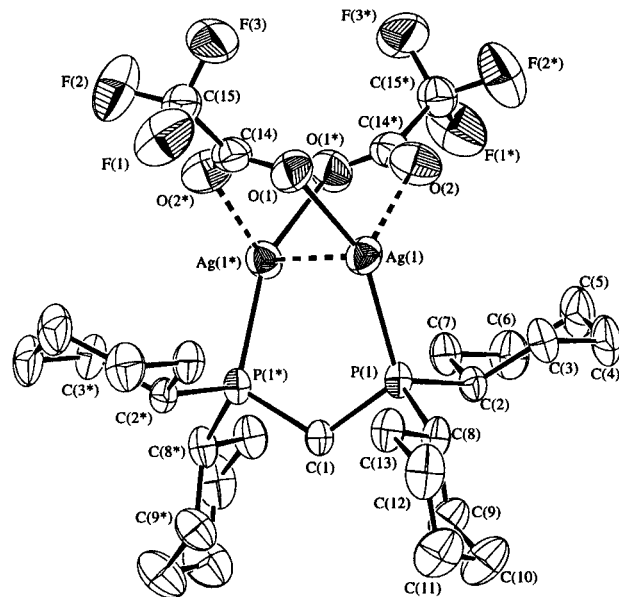


**Figure 3.** Perspective view of  $[\text{Ag}_2(\mu\text{-dcpm})(\mu\text{-O}_2\text{CCF}_3)_2]$ , **4** (40% thermal ellipsoids). Selected bond distances (Å) and angles (deg):  $\text{Ag}(1)-\text{Ag}(1^*)$  2.8892(9),  $\text{Ag}(1)-\text{O}(1)$  2.191(3),  $\text{Ag}(1)-\text{O}(2)$  2.446(4),  $\text{Ag}(1)-\text{P}(1)$  2.354(1),  $\text{O}(1)-\text{C}(14)$  1.240(6);  $\text{Ag}(1^*)-\text{Ag}(1)-\text{O}(1)$  90.0(1),  $\text{Ag}(1^*)-\text{Ag}(1)-\text{O}(2)$  74.4(1),  $\text{Ag}(1^*)-\text{Ag}(1)-\text{P}(1)$  88.96(3),  $\text{P}(1)-\text{Ag}(1)-\text{O}(1)$  152.3(1),  $\text{P}(1)-\text{Ag}(1)-\text{O}(2)$  113.5(1).

usually occur in a similar energy region. In this work, the aliphatic  $\text{PCy}_3$  and  $\text{dcpm}$  ligands are optically transparent in the UV region  $\lambda \geq 250$  nm. It is therefore feasible to probe the  $4d\sigma^* \rightarrow 5p\sigma$  transition originating from  $\text{Ag}(\text{I})-\text{Ag}(\text{I})$  interactions in the ground and excited states. In  $\text{CH}_2\text{Cl}_2$ , an intense UV-vis absorption band is observed for **2** and **3** at  $\lambda_{\text{max}}$  266 nm ( $\epsilon = 2.2 \times 10^4 \text{ dm}^3 \text{ mol}^{-1} \text{ cm}^{-1}$ ), and for **4** at  $\lambda_{\text{max}}$  243 nm ( $\epsilon = 1.3 \times 10^4 \text{ dm}^3 \text{ mol}^{-1} \text{ cm}^{-1}$ ; see Supporting Information).

(18) For example, see: (a) Zank, J.; Schier, A.; Schmidbaur, H. *J. Chem. Soc., Dalton Trans.* **1999**, 415–420. (b) Villanneau, R.; Proust, A.; Robert, F.; Gouzerh, P. *Chem. Commun.* **1998**, 1491–1492. (c) Ren, T.; Lin, C.; Amalberti, P.; Macikenas, D.; Protasiewicz, J. D.; Baum, J. C.; Gibson, T. L. *Inorg. Chem. Commun.* **1998**, 1, 23–26. (d) Chen, X. M.; Mak, T. C. W. *J. Chem. Soc., Dalton Trans.* **1991**, 1219–1222 and references therein. (e) Tsuda, T.; Ohba, S.; Takahashi, M.; Ito, M. *Acta Crystallogr.* **1989**, C45, 887–890. (f) Papisergio, R. I.; Raston, C. L.; White, A. H. *J. Chem. Soc., Chem. Commun.* **1984**, 612–613. (g) Ho, D. M.; Bau, R. *Inorg. Chem.* **1983**, 22, 4073–4079. (h) Chivers, T.; Parrez, M.; Schatte, G. *Angew. Chem., Int. Ed.* **1999**, 38, 2217–2219. (i) Robinson, F.; Zaworotko, M. J. *J. Chem. Soc., Chem. Commun.* **1995**, 2413–2414.

(19) Fu, W. F.; Chan, K. C.; Miskowski, V. M.; Che, C. M. *Angew. Chem., Int. Ed.* **1999**, 38, 2783–2785.

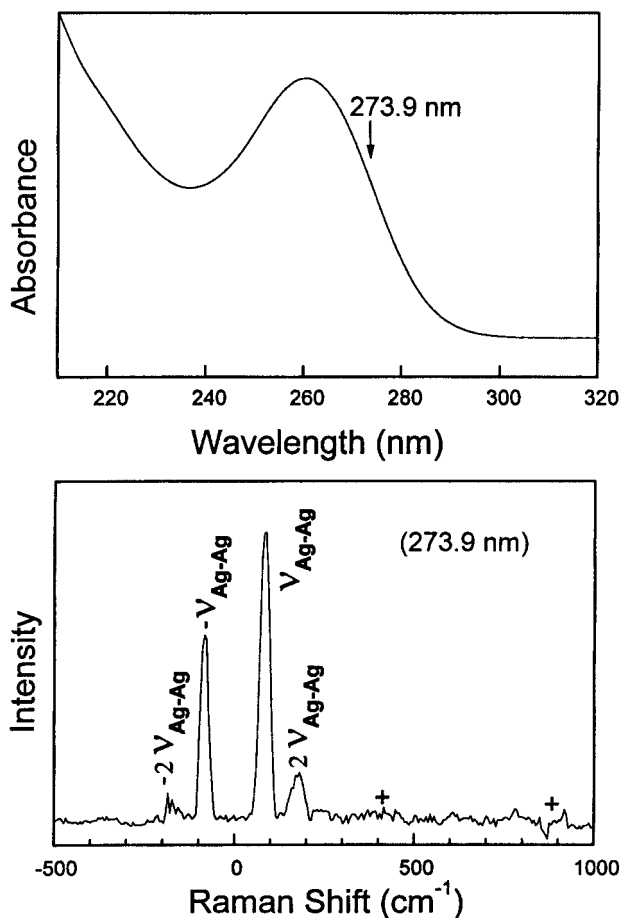


**Figure 4.** UV-vis absorption (top) and resonance Raman (bottom) spectra for  $[\text{Ag}_2(\mu\text{-dcpm})_2](\text{CF}_3\text{SO}_3)_2$  (**2**) in acetonitrile (solvent subtraction artifacts marked by +).

In contrast, the absorption spectra of **1** (monomeric in solution) and mononuclear  $[\text{Ag}(\text{PR}_3)_2]\text{ClO}_4$  ( $\text{R} = \text{Me}, \text{Cy}$ ) show  $\epsilon$  values below  $10^2$  at  $\lambda \geq 250$  nm. The high  $\epsilon$  values and profiles of the prominent absorptions are similar to the  $5d\sigma^* \rightarrow 6p\sigma$  transitions of  $\text{Au}_2(\text{P}-\text{P})_2^{2+}$  ( $\text{P}-\text{P} = \text{dppm}, \text{dcpm}$ ),<sup>20</sup> which exhibit weak  $\text{Au}(\text{I})-\text{Au}(\text{I})$  interactions in the ground state. Significantly, the intense band for **2** and **3** displays a slight blue shift to 261 nm in acetonitrile ( $\epsilon = 1.7 \times 10^4 \text{ dm}^3 \text{ mol}^{-1} \text{ cm}^{-1}$ ).<sup>21</sup> We suggest that weak solvent ( $\text{CH}_3\text{CN}$ ) $\cdots\text{Ag}$  contacts can disrupt the intramolecular  $\text{Ag}-\text{Ag}$  interaction, which would consequently affect the  $4d\sigma^* \rightarrow 5p\sigma$  transition. Previous reports have demonstrated that coordination of N-donor molecules, including acetonitrile, to the  $[\text{Cu}_2(\mu\text{-dppm})_2]^{2+}$  moiety results in very long  $\text{Cu}\cdots\text{Cu}$  interactions ( $>3.7 \text{ \AA}$ ).<sup>22</sup>

The 261 nm UV band for **2** in  $\text{CH}_3\text{CN}$  has been examined using resonance Raman spectroscopy, which confirms that it is metal-centered in nature. Figure 4 shows the 261 nm absorption and a resonance Raman spectrum obtained with 273.9 nm excitation: virtually all of the Raman intensity appears in the  $\text{Ag}-\text{Ag}$  stretch fundamental and overtone bands. It is evident that the transition is predominantly localized on the  $\text{Ag}-\text{Ag}$  bond. The depolarization ratio for the Stokes and anti-Stokes

fundamentals of the  $\text{Ag}-\text{Ag}$  stretch was measured. A value of 0.40 was obtained, which approaches the theoretical value of 0.33 for a  $nd\sigma^* \rightarrow (n+1)p\sigma$  transition. The observed  $\nu(\text{Ag}_2)$  at  $80 \text{ cm}^{-1}$  provides experimental support for that proposed for  $[\text{Ag}_2(\text{dmpm})_2](\text{PF}_6)_2$  ( $76 \text{ cm}^{-1}$ )<sup>23</sup> and  $[\text{Ti}[\text{Ag}(\text{CN})_2]]$  ( $\sim 88 \text{ cm}^{-1}$ )<sup>8b</sup> using nonresonant Raman techniques. The  $\nu(\text{Au}_2)$  value for the analogous  $\text{Au}_2(\text{dcpm})_2^{2+}$  species ( $88 \text{ cm}^{-1}$ )<sup>20</sup> is comparable to  $\nu(\text{Ag}_2)$  for **2** despite the higher atomic mass of gold. This is consistent with the fact that gold(I) has a greater tendency to undergo homoatomic attraction. The energy of the  $4d\sigma^* \rightarrow 5p\sigma$  transition for **2** and **3** also accounts for the difficulty in locating the corresponding transition in previous spectroscopic studies of polynuclear silver(I) compounds,<sup>24</sup> since the bridging or ancillary ligands in most instances absorb in a similar UV region. We note that the  $4d\sigma^* \rightarrow 5p\sigma$  transition for  $[\text{Ag}_2(\mu\text{-dmpm})_2]^{2+}$  appears at 256 nm ( $\epsilon = 1.3 \times 10^4 \text{ dm}^3 \text{ mol}^{-1} \text{ cm}^{-1}$ ) in  $\text{CH}_3\text{-CN}$ ; this minor blue shift compared to **2** and **3** is in accordance with a slightly longer  $\text{Ag}-\text{Ag}$  separation in  $[\text{Ag}_2(\mu\text{-dmpm})_2](\text{PF}_6)_2$  ( $3.041(2) \text{ \AA}$ ).<sup>13</sup>

The force constant  $F(\text{Ag}_2)$  estimated from the  $80 \text{ cm}^{-1}$   $\nu(\text{Ag}_2)$  value for **2** assuming a pure  $\text{Ag}_2$  stretch mode is  $0.203 \text{ mdyne \AA}^{-1}$ .<sup>25</sup> For nine binuclear  $\text{Ag}_2$  compounds, Harvey and co-workers<sup>26</sup> observed a good linear correlation between the  $\text{Ag}_2$  bond distance and  $\ln F(\text{Ag}_2)$  [ $r(\text{Ag}_2) = -0.284 \ln F(\text{Ag}_2) + 2.53$ ]. Our values for **2** fit very closely to the curve of the Harvey correlation, and provide further support for assignment of the resonance Raman bands of **2** to a  $\text{Ag}-\text{Ag}$  stretch. In addition, a resonance Raman intensity analysis study of **2** shows that the resonance Raman and absorption data can only be simulated accurately using a high excited-state frequency of ca.  $180 \text{ cm}^{-1}$  and a bond length change of ca.  $0.20 \text{ \AA}$ .<sup>27</sup> The apparent change to a substantially larger frequency reflects the expected  $\text{Ag}-\text{Ag}$  single bonded excited state for a  $nd\sigma^* \rightarrow (n+1)p\sigma$  transition. This is in agreement with previous studies by Omary and Patterson,<sup>28</sup> who proposed  $\text{Ag}-\text{Ag}$  bonded excited states to account for the solid-state photoluminescence of  $[\text{Ag}(\text{CN})_2]^-$  systems.

At 298 K, compounds **2** and **3** exhibit photoluminescence in the solid state at  $\lambda_{\text{max}}$  420 and 417 nm (lifetime  $\sim 0.5 \mu\text{s}$ ,  $E_{\text{ex}}$  270 nm), respectively.<sup>29</sup> The particularly large Stokes shifts of the solid emission maxima from the  $4d\sigma^* \rightarrow 5p\sigma$  absorption band in acetonitrile (ca.  $14500 \text{ cm}^{-1}$ ) indicate that the electronically excited  $[d\sigma^*, p\sigma]$  state may not be responsible for the luminescence. We have observed in our laboratory that changes in metal coordination, in both ground and excited states, can dramatically alter the emissions of related  $\text{Au}(\text{I})$ <sup>19</sup> and  $\text{Cu}(\text{I})$ <sup>30</sup> systems, while recent studies by Catalano and co-workers also

(23) Perreault, D.; Drouin, M.; Michel, A.; Miskowski, V. M.; Schaefer, W. P.; Harvey, P. D. *Inorg. Chem.* **1992**, *31*, 695–702.

(24) (a) Assefa, Z.; Patterson, H. H. *Inorg. Chem.* **1994**, *33*, 6194–6200. (b) Ford, P. C.; Vogler, A. *Acc. Chem. Res.* **1993**, *26*, 220–226. (c) Che, C. M.; Yip, H. K.; Li, D.; Peng, S. M.; Lee, G. H.; Wang, Y. M.; Liu, S. T. *J. Chem. Soc., Chem. Commun.* **1991**, 1615–1617. (d) Henary, M.; Zink, J. I. *Inorg. Chem.* **1991**, *30*, 3111–3112. (e) Vogler, A.; Kunkely, H. *Chem. Phys. Lett.* **1989**, *158*, 74–76.

(25)  $F(\text{Ag}_2) = \mu[2\pi c\nu(\text{Ag}_2)]^2$ ;  $\mu$  = reduced mass.

(26) (a) Perreault, D.; Drouin, M.; Michel, A.; Harvey, P. D. *Inorg. Chem.* **1993**, *32*, 1903–1912. (b) Harvey, P. D. *Coord. Chem. Rev.* **1996**, *153*, 175–198.

(27) See supporting information for full details.

(28) (a) Omary, M. A.; Patterson, H. H. *J. Am. Chem. Soc.* **1998**, *120*, 7696–7705. (b) Omary, M. A.; Patterson, H. H. *Inorg. Chem.* **1998**, *37*, 1060–1066.

(29) Complexes **2** and **3** display very weak emissions ( $\phi \leq 10^{-4}$ ) at  $\lambda_{\text{max}}$  380 (max) and  $\sim 590$  (broad) nm in acetonitrile at 298 K.

(30) Details will be published in due course: Mao, Z.; Che, C. M.; Phillips, D. L.

(31) Catalano, V. J.; Kar, H. M.; Garnas, J. *Angew. Chem., Int. Ed.* **1999**, *38*, 1979–1982. Also see ref 24d.

(20) Leung, K. H.; Phillips, D. L.; Tse, M. C.; Che, C. M.; Miskowski, V. M. *J. Am. Chem. Soc.* **1999**, *121*, 4799–4803.

(21) The perchlorate salt  $[\text{Ag}_2(\mu\text{-dcpm})_2](\text{ClO}_4)_2$  was also prepared and displays identical UV-vis absorption data.

(22) (a) Díez, J.; Gamasá, M. P.; Gimeno, J.; Tiripicchio, A.; Tiripicchio Camellini, M. *J. Chem. Soc., Dalton Trans.* **1987**, 1275–1278. (b) Li, D.; Che, C. M.; Wong, W. T.; Shieh, S. J.; Peng, S. M. *J. Chem. Soc., Dalton Trans.* **1993**, 653–654.

demonstrated similar findings for tetranuclear Ag(I) clusters.<sup>31</sup> In this report, close metal–anion contacts are observed in the crystal lattices of **2** and **3** (see above), and we therefore suggest that weak metal–anion interactions may play a role in the solid state emissions.

**Concluding Remarks.** Our current studies on  $[\text{M}_2(\mu\text{-dcpm})_2]^{2+}$  ( $\text{M} = \text{Ag}, \text{Au}^{19,20}$ ) afford a rare opportunity to directly compare Ag–Ag and Au–Au metallophilic bonding. Using the Raman-observed  $\nu(\text{M}_2)$  values [ $\text{M} = \text{Ag}$  ( $80 \text{ cm}^{-1}$ ),  $\text{Au}$  ( $88 \text{ cm}^{-1}$ )], the force constant assuming a pure  $\text{M}_2$  stretch mode is calculated<sup>25</sup> to be  $0.203 \text{ mdyne } \text{\AA}^{-1}$  for  $F(\text{Ag}_2)$  and  $0.449 \text{ mdyne } \text{\AA}^{-1}$  for  $F(\text{Au}_2)$ . These results may therefore serve as a useful indicator for comparing the bond strengths of Ag–Ag versus Au–Au interactions.

It is also pertinent to compare the  $nd\sigma^* \rightarrow (n+1)p\sigma$  transition energies of the  $[\text{Ag}_2(\text{dcpm})_2]^{2+}$  and  $[\text{Au}_2(\text{dcpm})_2]^{2+}$  complexes. The blue shift from 277 nm for  $\text{Au}_2$  to 261 nm for  $\text{Ag}_2$  is  $2213 \text{ cm}^{-1}$ , which approaches the corresponding value of  $2200 \text{ cm}^{-1}$  for the isoelectronic  $d^{10} [\text{M}_2(\text{dppm})_3]$  ( $\text{M} = \text{Pd}, \text{Pt}$ ) pair.<sup>3b</sup> This similarity is interesting and can be qualitatively ascribed to the difference in the  $nd \rightarrow (n+1)p$  energy gap of the free metal ions from second to third row transition metals. Quantitatively, this difference in energy gap is considerably more pronounced in the free metal ions ( $17200 \text{ cm}^{-1}$  for  $\text{Ag}/\text{Au}^{1a}$ ). It is well documented that Au(I) species exhibit metal–metal interactions

for both ground and excited states, and this is likely to be the situation for the Ag(I) system in view of the small energy difference between the  $nd\sigma^* \rightarrow (n+1)p\sigma$  transitions. Our results for the Ag(I) system suggest that  $nd\sigma^* \rightarrow (n+1)p\sigma$  excitation produces a silver–silver bonded excited state like for the Au(I) congener.<sup>20</sup> In summary, this article highlights the first spectroscopic verification for the existence of Ag(I)–Ag(I) attractive interactions in coordination compounds.

**Acknowledgment.** We are grateful to The University of Hong Kong, the Croucher Foundation of Hong Kong, and the Research Grants Council of the Hong Kong SAR, China [HKU 7298/99P and HKU 974/94P]. Dr. C. K. Chan is acknowledged for preliminary results in this work, and Dr. V. M. Miskowski is thanked for helpful discussions.

**Supporting Information Available:** Details of solvent treatment for photophysical studies, instrumentation, and emission measurements; ORTEP diagrams and tables of crystal data, atomic coordinates, calculated hydrogen coordinates, anisotropic displacement parameters, and bond distances and angles for **1–4**; UV–vis absorption spectra for **1** and **4**; resonance Raman intensity analysis study for **2** (PDF). This material is available free of charge via the Internet at <http://pubs.acs.org>.

JA9904890